



Optimal braking and steering control under split friction on curved roads

Downloaded from: <https://research.chalmers.se>, 2024-11-18 23:19 UTC

Citation for the original published paper (version of record):

Karyotakis, K., Yang, D., Jonasson, M. et al (2024). Optimal braking and steering control under split friction on curved roads. Lecture Notes in Mechanical Engineering: 604-610.

http://dx.doi.org/10.1007/978-3-031-70392-8_85

N.B. When citing this work, cite the original published paper.



Optimal Braking and Steering Control Under Split Friction on Curved Roads

Ektor Karyotakis^{1,2}(✉) , Derong Yang¹, Mats Jonasson³ ,
and Jonas Sjöberg² 

¹ Vehicle Energy and Motion Control, Volvo Car Corporation,
405 31 Gothenburg, Sweden

ektor.karyotakis@volvocars.com

² Department of Electrical Engineering, Chalmers University of Technology,
412 96 Gothenburg, Sweden

³ Department of Maritime and Mechanical Engineering,
Chalmers University of Technology, 412 96 Gothenburg, Sweden

Abstract. This paper aims to maximize deceleration on split friction roads by combining steering and individual wheel braking. For this, a previously tested optimization problem is adapted to curved roads. The optimal brake force and steering allocation is investigated as a function of the split friction asymmetry. Results show that low friction is more detrimental to maximum braking on the inner side of the curve due to load transfer. Finally, the paper showcases a control strategy for braking on split friction, which enhances safety and manoeuvrability in critical split friction scenarios.

Keywords: split · friction · optimization · cornering · curve · braking

1 Introduction

Split friction is an edge case of a slippery road where one side of the vehicle is on the regular road surface while the other is on a low-friction surface, like snow or fallen leaves. The road condition asymmetry creates an asymmetry in the brake forces, which in turn creates a yaw moment disturbance. The disturbance must be countered, typically by the driver, but can be abrupt and surprise the driver [8]. Making it autonomous would be beneficial to reduce accidents.

Contributions in literature have primarily focused on designing a controller for steering, assuming the ABS handles the brake control, as in [2, 10]. However, our research shows that using ABS on all wheels can be dangerous when there is a significant friction difference between the two vehicle sides. More advanced control solutions focus on designing the steering compensation and the brake control together [5, 9]. However, none of these have investigated the effects of friction on vehicle dynamics and maximum braking.

When braking under split friction, the maximum deceleration potential without deviating from the lane depends on the friction asymmetry [3]. In [7], the authors investigate the maximum deceleration potential on curved roads for

several steering/braking configurations and varying road friction coefficients. They showed a significant maximum deceleration potential reduction when the brake forces are constrained not to produce any yaw moment. Balancing the yaw moment on split friction braking is critical, but restricting the brakes implies longer stopping distances.

This paper analyses the maximum deceleration potential under split friction as a function of lateral acceleration and friction asymmetry. The resulting allocation of brake forces and steering can be used to design control algorithms better suited to varying friction. Inspired by this analysis, a control implementation is tested in simulation to show the potential.

2 Maximum Static Deceleration on Curved Roads

With the focus on maximising braking in a curve, an optimization problem (OP) is built upon a double-track vehicle model with combined slip and longitudinal and lateral load transfer; for details, see [1,3]. The focus of the OP on a high level is illustrated in Fig. 1.

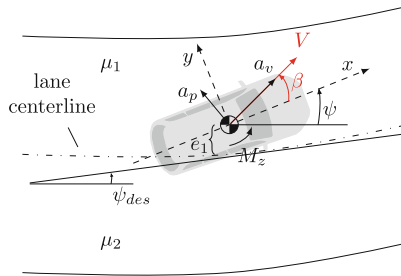


Fig. 1. Vehicle trajectory and orientation

The velocity vector is denoted with V , and its orientation, the side slip angle, with β . The vehicle's orientation is defined by the yaw angle ψ . In the static case of no dynamics, the acceleration along V , a_v , should be minimized. In contrast, the acceleration perpendicular to V , a_p , keeps the vehicle in the curve to a desired lateral acceleration $a_{p,des}$. Further, for a constant radius, yaw acceleration $\ddot{\psi}$ is unwanted; thus, the yaw torque $M_z = I_{zz}\ddot{\psi}$ should be zero. At the same time, the yaw rate $\dot{\psi}$ is chosen as a desired one.

For the desired lateral acceleration and yaw rate, the circular motion ones can be used, defined as

$$a_{p,des} = \frac{v_x^2}{R} \quad (1)$$

$$\dot{\psi}_{des} = \frac{v_x}{R} \quad (2)$$

where R is the road radius, and v_x the longitudinal speed. More advanced definitions can be obtained from [6].

The maximum static deceleration optimization problem is expressed as

$$\begin{aligned}
 & \min_q \quad a_v(q) \\
 & \text{s.t.} \quad a_p(q) = a_{p,des} \\
 & \quad \quad M_z(q) = 0 \\
 & \quad \quad \dot{\psi} = \dot{\psi}_{des} \\
 & \quad \quad F_{xi} = \frac{\sigma_{xi}(q)}{\sigma_i(q)} F_i(q) \\
 & \quad \quad F_{yi} = \frac{\sigma_{yi}(q)}{\sigma_i(q)} F_i(q) \\
 & \quad \quad \sqrt{F_{xi}^2 + F_{yi}^2} \leq k_F F_{\max,i}
 \end{aligned} \tag{3}$$

with $q = [\kappa_i, \delta, \beta]^\top$ the optimization variables, κ_i the longitudinal slip ratio, δ the steering angle. The control inputs are $u = [\kappa_i, \delta]^\top$, while $[\beta, \psi]$ are states. Equality constraints are needed for the forces $[F_{xi}, F_{yi}]$ to include the load transfer. Further, an inequality constraint is added for the friction circle, multiplied by a factor $0.95 < k_F < 1$ to avoid numerical instabilities at the friction peak and excessive slips.

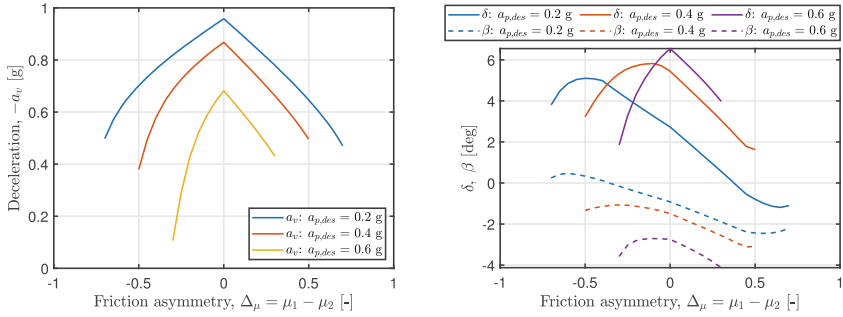
The solution to the OP (3) is static, without dynamics. In reality, as speed reduces, $a_{p,des}$ also reduces, and the vehicle brakes harder, giving a larger magnitude of a_v every instant. Instead, the solution can be seen as an upper limit to what deceleration can be achieved with the current speed and radius. For a straight road, the solution converges to a steady state instead as R becomes large and $1/R \rightarrow 0$ in (2). Next, the analysis of the OP is presented as a function of the friction difference between the vehicle sides.

3 Split Friction Effects

The *friction asymmetry* between the left (inner side for a left turn) μ_1 and right (outer) μ_2 vehicle side is defined as

$$\Delta_\mu = \mu_1 - \mu_2 \tag{4}$$

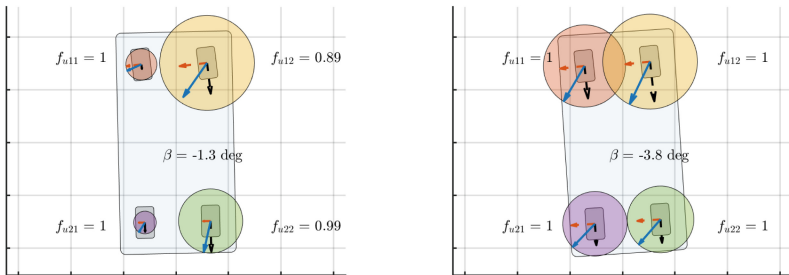
Several outputs from the OP (3) are depicted in Fig. 2 for several Δ_μ values. For positive Δ_μ , the outer curve side μ_2 varies, while the inner $\mu_1 = 1$, and vice versa for negative Δ_μ . The maximum deceleration potential is depicted in Fig. 2a. The curves are asymmetric. Less deceleration can be achieved when the inner side has lower friction ($\Delta_\mu < 0$) than when the outer side is on low friction ($\Delta_\mu > 0$). The main mechanism behind this is the lateral load transfer. The more lateral acceleration, the more pronounced the asymmetry becomes. The steering input and side slip angle are depicted in Fig. 2b. Some counter-steering is observed at large Δ_μ for the blue curve at low lateral acceleration. As lateral acceleration increases, the magnitude of steering inputs and side slip angles increase.



(a) Vehicle deceleration vs friction asymmetry (b) Vehicle steering and side slip angles vs friction asymmetry

Fig. 2. Vehicle deceleration, steering angle and side slip angle for several lateral acceleration values as a function of friction asymmetry

The optimal brake force and seeing allocations are depicted in Fig. 3 for two cases when the friction is low on the inner or outer curve side, respectively. The effect of load transfer is more important when the inner side has low friction, as the inner side friction circles are smaller, see Fig. 3a. Due to this mechanism, the side slip angle is also smaller, and the outer front circle moves away from the friction circle.



(a) Vehicle sketch for $\mu_1 = 0.6, \mu_2 = 1$ (b) Vehicle sketch for $\mu_1 = 1, \mu_2 = 0.6$

Fig. 3. Brake force/steering allocation for $a_{p,des} = 0.4$ g; The friction circles are scaled with the load; f_{ui} denotes how much of the friction circle is utilized

4 Vehicle Closed-Loop Simulations

Figure 4 shows the control logic. The human driver is replaced by a path-following *PD* steering controller using look-ahead measurements y from a vision system and is complemented by a feedforward steering angle based on friction. The brake controller controls the high-friction brakes to reduce excessive yaw torque using yaw rate $\dot{\psi}$ and the look-ahead measurement y as feedback. The low-friction side is controlled by the ABS. The details of the control logic are given in [4].

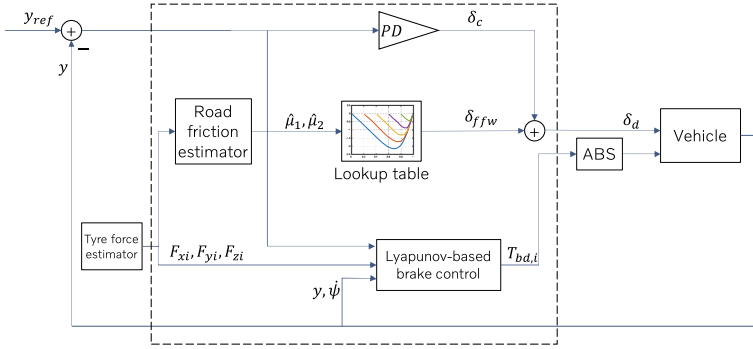
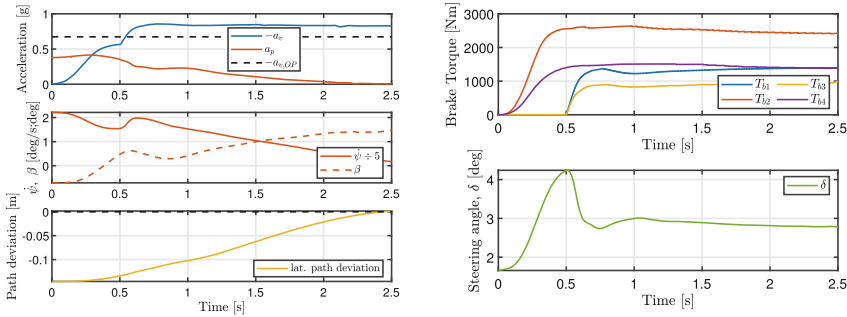


Fig. 4. Block diagram of control logic

Vehicle simulations are conducted in IPG CarMakerTM to validate the optimization, presented in Fig. 5. The simulation is performed for an initial speed of $V_0 = 70$ km/h and radius $R = 100$ m, corresponding to a lateral limit of $a_{p,des} \approx 0.4$ g. In Fig. 5a, the vehicle trajectory and motion states are depicted, while the states' targets are depicted with black dashed lines. The deceleration a_v surpasses the limit set by the OP $a_{v,OP}$ after a transient phase of about 0.7 s. The lateral acceleration a_p gradually decreases as a_v increases and velocity drops. At the same time, the yaw rate decreases linearly, as the side slip angle is almost constant, fluctuating around 1° . Also, the steering controller keeps path deviations small. The small side slip angle and path deviation at high deceleration show the vehicle's good manoeuvrability. In Fig. 5b, the control inputs are depicted. Interestingly, the ABS turns off the inner side brake torques up to 0.5 s due to excessive slip. It is also when the steering angle is at its peak.



(a) Vehicle states: accelerations, yaw rate & side slip angle, and path deviation (b) Control inputs: brake torques and steering wheel angle

Fig. 5. Closed loop simulation of a vehicle braking in a curve of $R = 100$ m on split friction with $\mu = [0.6 \ 1]$ and initial speed $V_0 = 70$ km/h

5 Conclusion

This paper presented a way to find the maximum braking during cornering on split friction roads. The maximum braking and the active front steering/differential brake torque allocations were investigated as a function of the friction difference between the vehicle's sides and the lateral acceleration. The analysis revealed that low friction on a curve's inner side is more dangerous than on the outer side due to the lateral load transfer. Further, a control logic was showcased that achieves good path-following and keeps the vehicle side slip small while achieving optimal deceleration. Future work includes using prior friction knowledge to predict optimal speed in a curve for varying friction road conditions.

References

1. Fors, V., Nielsen, L., Olofsson, B.: Models for Optimization of Vehicle Maneuvers. Vehicular Systems, ISY, Linköping University (2023)
2. Hebden, R.G., Edwards, C., Spurgeon, S.K.: Automotive steering control in a split- μ manoeuvre using an observer-based sliding mode controller. *Veh. Syst. Dyn.* **41**, 181–202 (2004). <https://doi.org/10.1076/vesd.41.3.181.26511>
3. Karyotakis, E., Jonasson, M., Yang, D., Sjöberg, J.: Minimizing stopping distance on split friction via steering and individual wheel braking optimization. In: The 28th IAVSD Symposium on Dynamics of Vehicles on Roads and Tracks (2023)
4. Karyotakis, E., Jonasson, M., Yang, D., Sjöberg, J.: Minimum stopping distance on split friction roads via joint control of steering and individual wheel braking. *Veh. Syst. Dyn.* (2024, to be submitted)
5. Mirzaeinejad, H., Mirzaei, M., Kazemi, R.: Enhancement of vehicle braking performance on split- μ roads using optimal integrated control of steering and braking systems. *Proc. Inst. Mech. Eng. Part K J. Multi-body Dyn.* **230**, 401–415 (2016)
6. d'Andrea Novel, B., Ellouze, M.: Tracking with stability for a vehicle braking in a corner. In: Proceedings of the 40th IEEE Conference on Decision and Control (Cat. No. 01CH37228), vol. 5, pp. 4427–4432. IEEE (2001)
7. Peng, H., Hu, J.S.: Traction/braking force distribution for optimal longitudinal motion during curve following. *Veh. Syst. Dyn.* **26**, 301–320 (1996). <https://doi.org/10.1080/00423119608969313>
8. Tagesson, K., Jacobson, B., Laine, L.: Driver response to automatic braking under split friction conditions. In: Proceedings of the 12th International Symposium on Advanced Vehicle Control (AVEC), pp. 666–671 (2014)
9. Xue, Z., Li, C., Wang, X., Li, L., Zhong, Z.: Coordinated control of steer-by-wire and brake-by-wire for autonomous emergency braking on split- μ roads. *IET Intell. Transp. Syst.* **14**, 2122–2132 (2020)
10. Yu, L., Zheng, S., Dai, Y., Abi, L., Liu, X., Cheng, S.: A feedback-feedforward steering controller designed for vehicle lane keeping in hard-braking manoeuvres on split- μ roads. *Veh. Syst. Dyn.* **60**, 1763–1787 (2022)

Open Access This chapter is licensed under the terms of the Creative Commons Attribution 4.0 International License (<http://creativecommons.org/licenses/by/4.0/>), which permits use, sharing, adaptation, distribution and reproduction in any medium or format, as long as you give appropriate credit to the original author(s) and the source, provide a link to the Creative Commons license and indicate if changes were made.

The images or other third party material in this chapter are included in the chapter's Creative Commons license, unless indicated otherwise in a credit line to the material. If material is not included in the chapter's Creative Commons license and your intended use is not permitted by statutory regulation or exceeds the permitted use, you will need to obtain permission directly from the copyright holder.

